Experimental study of resonant photoemission in the metals V, Cr, Mn and Co

1997 J. Phys.: Condens. Matter 9 6533

(http://iopscience.iop.org/0953-8984/9/31/007)

J. Phys.: Condens. Matter **9** (1997) 6533–6542. Printed in the UK PII: S0953-8984(97)81023-5

Experimental study of resonant photoemission in the metals V, Cr, Mn and Co

T Kaurila, J Väyrynen and M Isokallio

Laboratory of Materials Science, Department of Applied Physics, University of Turku, FIN-20014 Turku, Finland

Received 16 January 1997, in final form 2 April 1997

Abstract. We have studied the resonant photoemission of the valence band in V, Cr, Mn and Co transition metals using synchrotron radiation excitation near the 3p ionization thresholds. The effect of the 3p–3d interaction reaches maximum strength in Cr and Mn. On the other hand, the contribution related to the atomic Fano resonance goes to a minimum in Mn and increases rapidly on moving to Co. This behaviour is also reflected in the values of the effective Coulomb hole–hole interaction which we have calculated from experimental spectra. Furthermore, we have investigated when the $M_{2,3}VV$ Auger transition appears in the vicinity of the 3p ionization thresholds. Our results reveal that V, Cr and Co do not show the so-called subthreshold Auger emission whereas it can possibly be observed in Mn. However, we attribute the unusual appearance of the Auger peak to the wide valence band of Mn rather than the 3p–3d resonance.

1. Introduction

The activity in resonant photoemission experiments on the 3d transition metals was highest in the last decade but some curiosity regarding this field still persists [1–4]. The series V, Cr, Mn and Co is interesting since in the ground states their atomic electron configurations are d^3s^2, d^5s^1, d^5s^2 and d^7s^2, respectively. Thus, chromium represents a deviation in the filling order. Moreover, vanadium has three d electrons in the valence band and cobalt lacks three d electrons from the closed d shell. According to calculations, the width of the 3p–3d resonance should be much broader in V and Cr than in Mn and Co [5].

The resonant behaviour of the valence band near the 3p ionization threshold has been studied quite extensively for Cr but only few papers have been published on V [1, 6–9]. Also, we did not find any resonant profile for metallic Mn and Co. Some work has also been carried out by means of electron energy-loss spectroscopy (EELS) [10–14]. Because the excitations of an EELS experiment rarely obey the dipole selection rules observed in photon excitation, it is difficult to obtain the partial photoionization cross section from EELS measurements. Photoemission satellites, appearing in valence bands and relating to the resonant excitations in the vicinity of the 3p threshold, have been under debate for several 3d transition metals [8, 15, 16]. Although it has been verified that nickel is the only 3d element which can possess valence band satellites, the discussion has shed further light on the resonant photoemission phenomenon. Moreover, the resonant photoemission of some metal cations (V, Mn) in transition metal oxides has been investigated [17–19].

Resonant photoemission can be described as an interference between the direct photoemission and the recombination of an excited state, corresponding to autoionization. In

0953-8984/97/316533+10$19.50

the atomic one-electron notation, this means that the normal 3d photoemission $3p^6 3d^N 4s^2 + h\nu \rightarrow 3p^6 3d^{N-1} 4s^2 + e^-$ and the decay of the core excitation as $3p^5 3d^{N+1} 4s^2 \rightarrow 3p^6 3d^{N-1} 4s^2 + e^-$ interfere. The latter transition becomes possible as a 3p electron is excited initially into an unoccupied state above the Fermi level. Since an atom ends up in the same final state in both processes, we can regard the processes as coherent. The interaction of these two de-excitation channels causes the intensity of the 3d band to decrease at photon energies close to the 3p threshold. On the other hand, above the threshold the intensity of the 3d peak is enhanced significantly.

In addition to the autoionization, there exists another decay mechanism for a 3p hole state. If an excited 3p electron is delocalized or emitted, an ordinary $M_{2,3}M_{4,5}M_{4,5}$ Auger emission, i.e. the super-Coster–Kronig transition (sCK) in this case, will be able to take place with photon energies equal to or higher than the 3p threshold energy. Consequently, the Auger emission and the autoionization are the competing decay events of a 3p hole state.

In this paper, we shall consider how the resonant profile of the valence band changes as the occupancy of the 3d band increases from three d electrons to seven d electrons in the first-row transition metals. We shall also study the appearance of the sCK Auger peaks close to the 3p edges. In particular, we shall concentrate on resolving whether the Auger transition can occur below the 3p threshold—named a subthreshold Auger emission. Finally, we shall estimate the effective Coulomb interaction U_{eff} between two holes in the valence band of these metals.

2. Experimental procedure

The experiments were carried out at the beamline 41 (BL41) at the MAX synchrotron radiation facility in Lund, Sweden. BL41 has been equipped with a toroidal grating monochromator and an angle-resolved hemispherical electron energy analyser described elsewhere [20, 21]. The measurements were performed over the photon energy range 20–150 eV when the total resolution, determined from the widths of the Fermi level, varied from 0.4 eV to 0.6 eV. Good statistics is far preferable to high resolution in this kind of study.

The energy calibration of the spectra was done by means of derived Fermi edges. We also measured the absolute value of the photon energy with the aid of second-order light and the Pb 5d levels of PbS. The spectra were recorded at normal emission with respect to the sample surfaces, and the angle between the incident photon beam and the detection direction of the analyser was kept at 55°.

We prepared our samples, thick bulk-like layers, by evaporating high-purity metals onto mechanically polished gold substrates. Evaporators had been constructed by wrapping an electrically heating tungsten filament around a metal source that was a wire for V and Co, a clump for Cr and a flake in the case of Mn. To avoid surface contamination, the evaporators were outgassed carefully before the depositions, and the evaporations were done as quickly as possible [22]. The base pressure was 5×10^{-10} mbar during the experiments. The cleanness of the surfaces was checked by monitoring the 2p peak of oxygen located about 6 eV below the Fermi edge. If the peak did not appear in the spectra, the surface was regarded as free from contaminants. This assumption is based on the fact that the photoionization cross section of the O 2p level is considerable below photon energies of 100 eV [23]. If we observed the surface to be contaminated, we evaporated a new thick layer.

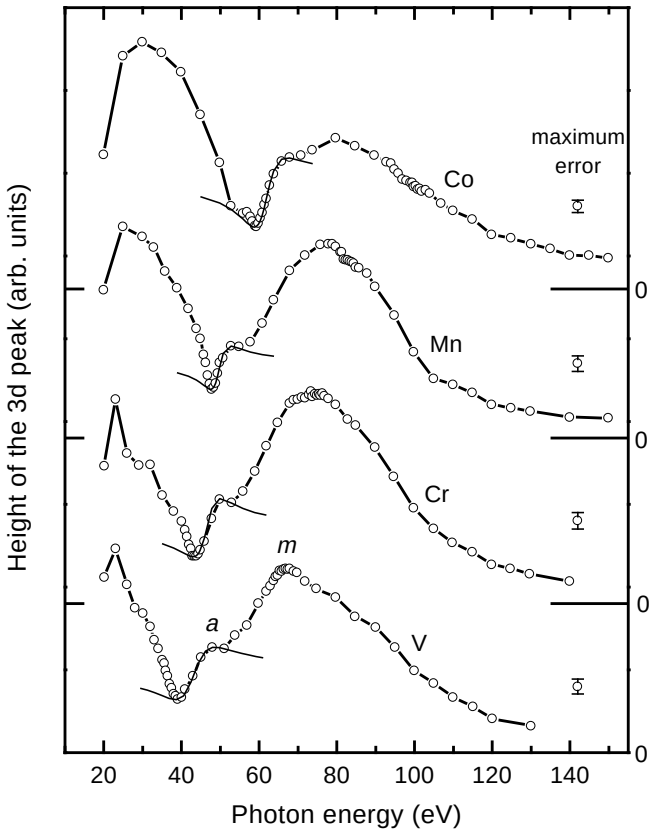

Figure 1. The resonant profiles of V, Cr, Mn and Co. The binding energy positions from which the profiles have been extracted are 0.6, 1.1, 0.75 and 0.5 eV, respectively. Short solid lines close to minima are the fitted Fano profiles, representing the atomic contribution in the 3p–3d resonance.

3. Results and discussion

The partial photoionization cross sections of the upper 3d band in V, Cr, Mn and Co are shown in figure 1, corresponding to the binding energies 0.6, 1.1, 0.75 and 0.5 eV, respectively. Since we measured sequential photoelectron spectra as functions of the photon energy, we had to extract the heights of the valence bands from the spectra to obtain the resonant profiles. Thus, the curves are consistent with constant-initial-state (CIS) spectra excluding the effects of white noise subtracted prior to the profiling. We assumed the white-noise background to be uniform and estimated its intensity according to the counts above the Fermi level. The contribution of inelastically scattered electrons remains small in the background, as the positions considered are located very near the Fermi edge. The intensity of the raw spectra was normalized with respect to the incident photon flux by a method described elsewhere [2].

In table 1 we have given a few main parameters connected to the resonant profiles of the metals studied. The weighted mean binding energies of the 3p components have been obtained by means of a curve-fitting program (table 2). $E_{\min}$ and $E_{\max}$ denote photon energies at which the interference is destructive and constructive, respectively, resulting in a

Table 1. The most important parameters related to the 3p–3d resonance. E_B is the mean binding energy, and E_{min} and E_{max} denote the photon energies at which the minimum and maximum occur in the profile. h refers to the height of the 3d band, and I_{atom} and W are the relative proportion of the atomic Fano resonance and the full width at half-maximum value at constructive resonance, respectively.

	V	Cr	Mn	Co	Error
E_B(3p) (eV)	37.1	42.4	47.3	59.5	±0.1
E_{min} (eV)	39.1	43.5	47.9	59.2	±0.3
E_{max} (eV)	67	74	77	80	±2
h_{max}/h_{min}	3.5	4.4	3.9	2.4	±0.2
I_{atom} (%)	39	35	29	79	±2
W (eV)	38	36	43	36	±2

dip and a maximum in the profile, respectively. h refers to the height of the 3d band. I_{atom} corresponds to the relative proportion of the atomic Fano resonance. We have calculated it from the expression $(h_{atom} - h_{min})/(h_{max} - h_{min})$, where h_{atom} is the height of the shoulder on the left-hand side of the main maximum, labelled 'a' in figure 1. W is the full width at half-maximum at resonance, as the intensity level of the minimum is used as a base-line reference.

The resonant profiles of figure 1 agree well with the characteristic Fano shape: a minimum close to an excitation threshold and the following maximum as a result of the interference between the wavefunctions of an autoionization electron and an ejected photoelectron. In the minimum, i.e. for destructive interference, the wavefunctions are out of phase. When approaching the maximum, the wavefunctions shift to the same phase, enhancing the total yield. The common, decreasing tendency toward higher photon energies is an inherent property due to the partial photoionization cross section of the valence band, which becomes weaker as the excitation energy increases.

Despite the similarities with the atomic Fano resonance, two prime differences can also be noticed compared to the resonant behaviour of free atoms. First of all, the onset of the resonance is delayed, reaching a maximum far above the 3p threshold. Secondly, the resonance can occur over an unusually broad energy range. Both the delay and the width of the resonance process can be explained qualitatively by the existence of unoccupied electron states above the Fermi level. They allow shake-up transitions from the valence band to empty states simultaneously with the excitation of a 3p core electron. As unoccupied electron levels expand to bands in metals, any amount of energy loss up to a certain limit is available for shake-up satellites, making the loss distribution continuous across several tens of electron volts.

The resonant profiles reveal both atomic and metallic contributions, indicated by 'a' and 'm' in the profile of V, in the 3p–3d resonance. Hence it is easy to discover how their intensity ratio will change as the number of 3d electrons increases. The shoulder on the left-hand side of the maximum (a), immediately above the minimum, represents atomic effects. It corresponds to the atomic resonance in the Fano interaction [6]. In order to establish the positions of the atomic parts in figure 1, they were fitted by Fano profiles (short solid lines) which produced q-parameters of 0.9, 1.0, 0.8 and 0.7 for V, Cr, Mn and Co, respectively. The maximum itself (m) can be connected to the metallic nature that depends on the density of empty electron bands. Shake-up excitations to unoccupied bands delay the onset of the 3p–3d interaction and stretch the resonant range as discussed above. In moving from V to Mn the atomic effects reduce gradually until they increase suddenly in Co, in which these

two contributions are already nearly equal.

The minimum of the 3p–3d resonance occurs clearly above the threshold in V, Cr and Mn, whereas it is slightly below the 3p edge in Co. Thus, the position of the destructive interference approaches the 3p threshold as the occupancy of the valence band increases. The location of the maxima varies nearly linearly with the atomic number. Only V resonates at a lower photon energy than the general trend suggests. The behaviour of the minima and maxima can be assigned to the location and density of unoccupied states, respectively. The dominant structures of the unoccupied 3d band come closer to the Fermi level and cross it in Ni [26], meaning that the required excitation energy for going from the 3p core level to an empty state approaches the 3p ionization energy. On the other hand, when going from V to Co, the valence band fills, which causes there to be fewer empty electron states per atom. The lack of suitable excitation states reduces the probability of shake-up losses, resulting in more atomic character of the 3p–3d interaction. Consequently, the position of the maximum also approaches the 3p threshold.

The strength of the resonance described by $h_{\max}/h_{\min}$ increases to a maximum in Cr and decreases significantly in moving to Co. However, the overall widths of the 3p–3d resonance are quite similar for all of the metals studied except Mn, whose resonant range is about 5 eV broader. The values obtained disagree with those calculated by Davis and Feldkamp, since their work predicts the width of the resonant region to be unambiguously wider in Cr than in Mn and Co [5]. The most probable reason for the different results may be the fact that Davis and Feldkamp interpreted the 3p excitation spectra with an atomic model.

The origin of the small hump that can be especially clearly seen in the resonant profile of V and Cr close to 30 eV is unknown so far. But we suggest that it might arise from the normalization of the photon flux, for the yield spectrum of gold has a quite intense peak at around a photon energy of 30 eV. Our proposal is also supported by the work of Barth *et al* who have recorded the same feature for the elements from Ca to Cr [6]. We cannot find any reason for the observed structure being present at the same excitation energy in Ca and several 3d metals. Thus, we have concluded that this feature is related to a measurement system or a normalization procedure.

An interesting question regarding the metals investigated is that of whether the sCK transition can occur below the 3p threshold. Walker *et al* have studied the $M_{2,3}M_{4,5}M_{4,5}$ Auger emission in iron and found it to appear even below the 3p excitation edge [24]. Moreover, subthreshold Auger emission within the lifetime broadening of the core hole has been predicted by Yafet [25]. We examined earlier the subthreshold Auger event in titanium and iron, but our studies did not support the existence of the phenomenon in either of the metals [4, 2]. However, in the case of iron we were not able to determine definitely when the MVV peak appears because the energy steps near the 3p threshold in our measurements were too rough.

Figure 2 shows the onsets of the difference energy distribution curves (DEDCs) on the higher-kinetic-energy side for V, Cr, Mn and Co. The DEDCs, corresponding to the normal sCK Auger peaks, have been obtained by subtracting a reference energy distribution curve (REDC) from the valence band spectra close to the 3p excitation threshold. As the REDCs, we used the valence band spectra which were measured below the 3p excitation thresholds with photon energies of 36.5, 41.0, 46.2 and 57.8 eV, respectively. Prior to the subtraction, the REDCs and the valence band spectra were scaled to the same height according to the maxima of the valence bands. Also, since the intensity of the Auger peaks changes with the excitation energy, we normalized the DEDCs, also afterwards, to get similar intensities at higher binding energies. This helps us to resolve more exactly where the Auger peaks

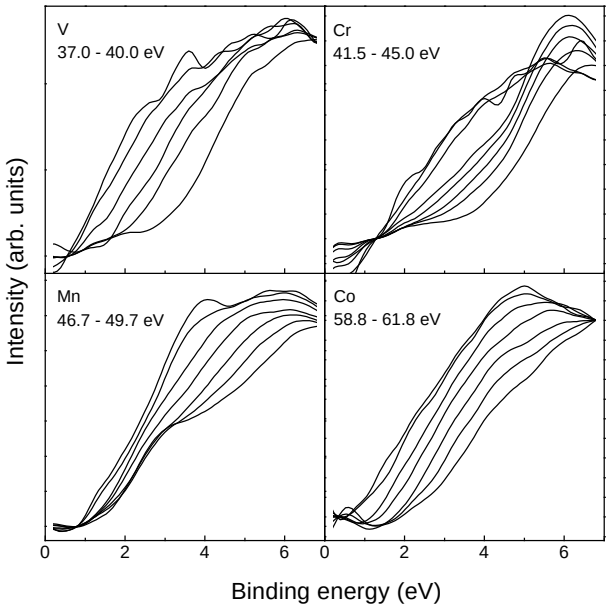

Figure 2. The onsets of the difference energy distribution curves (DEDC) for V, Cr, Mn and Co in the vicinity of the 3p thresholds. The method by which the DEDCs have been generated is described in the text. The photon energies, increasing from left to right, are shown under the elements. The photon energy step between two curves is 0.5 eV, except for V where it is 1.0 eV when going from 39.0 eV to 40.0 eV.

Table 2. The binding energies of the 3p and 3s core levels, the spin–orbit splitting of the 3p peaks and the kinetic energy of the $M_{2,3}M_{4,5}M_{4,5}$ Auger peaks. All of the energies have been given with respect to the Fermi level, in eV. Also, the positions of the valence band maxima and Coulomb hole–hole interaction potentials $U_{\rm eff}$ are shown.

	V	Cr	Mn	Co	Error
$E_B(3p_{3/2})$	36.9	42.1	47.0	59.1	±0.1
$E_B(3p_{1/2})$	37.6	43.0	47.8	60.3	±0.1
$\Delta_{\rm spin-orbit}$	0.7	0.9	0.8	1.2	±0.1
$E_B(3s)$	65.9	74.1	82.0	101.6	±0.2
E_K(MVV)	33.6	37.8	42.8	54.2	±0.3
$E_B(3d_{\rm max})$	0.6	1.3	1.8	0.6	±0.1
$U_{\rm eff}$	2.3	2.0	0.9	4.1	±0.4

appear and what their shifts in energy are as the excitation energy increases. The post-scaling positions vary between 7 eV and 8.5 eV, depending on the elements.

As figure 2 reveals, V, Cr and Co do not indicate subthreshold Auger emission, whereas it may be observed in the case of Mn. The appearance of the Auger emission can be recognized as the shift of the onset of the DEDC with excitation energy. In other words, when the onset of the DEDC moves by the same amount as the photon energy is varied, the moving peak can be connected to the Auger transition, shifting with the photon energy on the binding energy scale. Moreover, if the shifting starts below the 3p threshold, this indicates subthreshold Auger emission. To verify the excitation thresholds, we measured the binding energies of the 3p core levels, and the values obtained are given in table 2.

The appearance of the MVV peaks occurs at photon energies slightly higher than the 3p excitation thresholds in the cases of V, Cr and Co. However, the Auger peak of Mn already appears slightly below 47.0 eV—that is, the 3p threshold energy—and starts to move toward higher binding energies. Mn has a permanent structure near 3 eV, caused by another separate valence band peak resonating differently from the peak just below the Fermi level. One reason for the different resonant behaviour is probably the type of 3d electron: the peak of 0.5 eV mainly consists of the t_{2g} contribution, whereas the lower one consists mostly of the e_g component [26]. The dominating structures at around 6 eV originate partly as a result of the normalization before the subtraction of the REDCs. This is because the intensity of the valence band passes through a minimum in the destructive interference. At the same time, the intensity of the lower part of the spectra close to 6 eV is nearly constant. The intensity of this region is mainly produced by inelastically scattered electrons and surface impurities.

So far, we do not know what the ultimate reason is for the potential subthreshold Auger emission in Mn and in Fe. On the one hand, the irregular Auger behaviour may relate to half-filled 3d shells: $3d^5 4s^2$ and $3d^6 4s^2$ in atomic notation. On the other hand, why do we not detect the subthreshold event in Cr with the $3d^5 4s^1$ configuration?

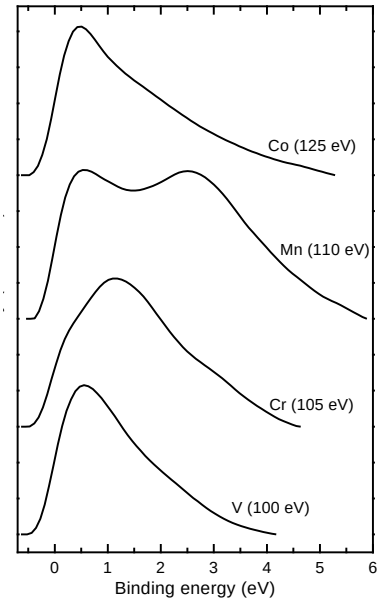

Figure 3. The valence bands of V, Cr, Mn and Co after removing the linear background. The excitation energies are shown in parentheses.

If we consider the widths of the valence bands, we may be able to explain the exceptional Auger emission. For this purpose, we have determined values of the full width at half-maximum (FWHM) from the experimental valence bands (figure 3) far above the 3p–3d interaction region. Before extracting the FWHM values, the linear background was removed. The background was fixed at a zero level above the Fermi edge and in the position where the intensity is set at a constant level on the higher-binding-energy side. The widths are 2.0, 2.6, 4.0 and 2.0, respectively. For Fe, we have measured a FWHM of 3.7 eV previously [2]. Thus, the valence bands of Mn and Fe are considerably broader than those of the other metals investigated. Since the sCK Auger distribution can be represented roughly by

the autoconvolution of the occupied valence band, neglecting transition probabilities, the broadening of the MVV peak is much stronger for elements with wide valence bands [27]. Now, if any matrix element connects the excitation channel and the decay channel close to the excitation threshold, the broadening of the sCK peak may cause the onset of the Auger peak to become visible even below the 3p threshold energy. The broadening of the Auger distribution also depends on the lifetime of an initial hole state. But, in Mn and Fe we can ignore the initial-state effect, owing to the narrow 3p peaks with respect to the valence bands. Consequently, we propose that the potential subthreshold Auger phenomena in Mn and Fe probably originate from the intrinsic widths of the valence bands and are not produced by the 3p–3d interaction. However, to establish this with absolute certainty, more detailed study is needed to confirm the existence of the subthreshold Auger emission in Mn and Fe as well as to establish its origin.

In addition to the valence band spectra, we measured the 3p and 3s core levels and the $M_{2,3}VV$ Auger distributions far above the excitation thresholds. The numerical results have been summarized in table 2. Because the Auger peaks were located against a high level of background, arising from inelastically scattered electrons, we used third-degree polynomials to remove the influence of the inelastic background. The excitation energies are 95 eV for V and Cr, 100 eV for Mn and 140 eV in the case of Co. The binding energies of the $3p_{1/2}$ and $3p_{3/2}$ levels have been obtained from the spectra using a curve-fitting program. Prior to fitting, we subtracted the integrated background, which is analogous with the Shirley model.

Our binding energies are in very good agreement with the values published by Fuggle and Mårtensson [28]. Only the values of the 3s core levels are systematically shifted—and then only slightly—to lower energies in our work. We did not find any paper in which the spin–orbit splitting of the 3p peaks was reported. This might be due to the fact that the spin–orbit splitting is not resolved in the photoemission spectra of the 3d metals studied. The splitting expands when the atomic number of the element increases, as we would expect. Our values for the sCK transitions are the kinetic energies in the real peak maxima referred to the Fermi level, since the sCK distributions each consist of one primary peak. The Auger energies agree well with the values observed in the electron energy-loss measurements in references [12], [13] and [14].

Finally in this section, we consider the effective Coulomb interaction U_{eff} between two valence band holes. We can estimate U_{eff} by means of the relation $U_{\mathrm{eff}} = E_{3\mathrm{p}} - 2E_{3\mathrm{d}} - E_{\mathrm{Auger}}$, in which $E_{3\mathrm{p}}$, $E_{3\mathrm{d}}$ and E_{Auger} are the binding energies of the 3p level and the valence band, and the kinetic energy of the sCK transition referred to the Fermi level. In order to achieve as high an accuracy as possible, we have used the energy positions at which the 3p photoelectron peaks and the valence bands have maximum intensity, except for the valence band of Mn owing to its double-peak structure (table 2). We base our method on the fact that the maxima of the peaks probably produce the main contribution to the Auger distributions even when one neglects matrix elements.

The calculated hole–hole interaction energies have been presented in table 2. In the literature, the value of U_{eff} varies from -0.1 eV for Cr up to 3.7 eV for Co [15, 29–31]. In particular, Antonides *et al* and de Boer *et al* have obtained less Coulomb repulsion for 3d holes than we did. Yin *et al* and Ramsey and Russell arrived at values similar to ours. If the determination is done with the aid of an Auger peak, the result is very sensitive to what value is selected for the Auger energy. Also, the equation used assumes the Auger transition to be a one-electron process that contains the total effects of intra-, inter- and extra-atomic relaxation. The results for U_{eff} suggest the degree of localization of the 3d holes to be less in the metals with half-filled 3d subshells. This also means that the atomic effects in the 3p–3d interaction should be weaker in Cr and Mn than in V and Co. In

comparing the effective Coulomb hole–hole interaction of the metals to the observed I_{atom}-values, associated with the strength of the atomic resonance, we find excellent agreement between U_{eff} and I_{atom}. Hence the similar behaviour of U_{eff} and I_{atom} confirms further that the shoulder on the left-hand side of the maximum in the resonant profiles can indeed be ascribed to atomic effects.

4. Conclusions

We have studied the resonant photoemission in V, Cr, Mn and Co metals in the vicinity of the 3p excitation thresholds. The 3p–3d resonance shows the typical Fano shape, excluding the delay of the resonance and the stretching of the resonant region. The strength of the 3p–3d interaction is strongest in Cr. The influence of atomic effects in the resonance reduces gradually from V to Mn, until they again play an important role for Co. This behaviour is also suggested by the effective Coulomb hole–hole interaction of these metals. In addition to the resonant photoemission, we examined the subthreshold Auger emission in the metals. Our research reveals that the sCK peak can appear even below the excitation threshold in manganese, whereas the other elements do not show a corresponding feature. However, we assign the subthreshold Auger event to the wide valence band of Mn rather than the influence of the 3p–3d resonance. Similarly, we can explain the appearance of the sCK peak below the 3p threshold in iron reported earlier.

Acknowledgments

We would like to thank the staff of the MAX Laboratory for their assistance and helpful advice. We also acknowledge the Academy of Finland for financial support.

References

[1] Säisä L, Kaurila T and Väyrynen J 1992 *Solid State Commun.* **83** 407
[2] Kaurila T, Säisä L and Väyrynen J 1994 *J. Phys.: Condens. Matter* **6** 5053
[3] Lópes M F, Laubschat C, Gutiérrez A, Höhr A, Domke M, Kaindl G and Abbate M 1994 *Z. Phys.* B **95** 9
[4] Kaurila T, Väyrynen J and Isokallio M 1996 *J. Electron Spectrosc. Relat. Phenom.* **82** 165
[5] Davis L C and Feldkamp L A 1976 *Solid State Commun.* **19** 413
[6] Barth J, Gerken F and Kunz C 1985 *Phys. Rev.* B **31** 2022
[7] Bader S D, Zajac G, Arko A J, Brodsky M B, Morrison T I, Zaluzec N, Zak J, Benbow R L and Hurych Z 1986 *Phys. Rev.* B **33** 3636
[8] Chandesris D, Lecante J and Petroff Y 1983 *Phys. Rev.* B **27** 2630
[9] Barth J, Gerken F, Kobayashi K L I, Weaver J H and Sonntag B 1980 *J. Phys. C: Solid State Phys.* **13** 1369
[10] Zajac G, Bader S D, Arko A J and Zak J 1984 *Phys. Rev.* B **29** 5491
[11] Chiarello G, Formoso V, Caputi L S and Colavita E 1987 *Phys. Rev.* B **35** 5311
[12] del Pennino U, Calandra C, Grandi L, Mariani C and Valeri S 1987 *Phys. Scr.* **35** 54
[13] Cornaz A, Erbudak M, Aebi P, Stucki F and Vanini F 1987 *Phys. Rev.* B **35** 3062
[14] Ramsey M G and Russell G J 1985 *Phys. Rev.* B **32** 3654
[15] Ramsey M G and Russell G J 1985 *Appl. Surf. Sci.* **22/23** 206
[16] Raaen S and Murgai V 1987 *Phys. Rev.* B **36** 887
[17] Smith K E and Henrich V E 1988 *Phys. Rev.* B **38** 9571
[18] Shin S, Suga S, Taniguchi M, Fujisawa M, Kanzaki H, Fujimori A, Daimon H, Ueda Y, Kosuge K and Kachi S 1990 *Phys. Rev.* B **41** 4993
[19] Lad R J and Henrich V E 1988 *Phys. Rev.* B **38** 10 860
[20] MAX Laboratory Synchrotron Radiation Group 1987 *MAX Laboratory Activity Report* p 46
[21] Karlsson U O, Andersen J N, Hansen K and Nyholm R 1989 *Nucl. Instrum. Methods* A **282** 553

[22] Kaurila T 1996 Evaporation of Ti film and its contamination in ultra-high vacuum *Internal Report Series of the Department of Applied Physics of the University of Turku* TURKU-SFL-R15, ISBN 951-29-0791-7, ISSN 0789-1822
[23] Yeh J J and Lindau I 1985 *At. Data Nucl. Data Tables* **32** 1
[24] Walker K-H, Kisker E, Carbone C and Clauberg R 1987 *Phys. Rev.* B **35** 1616
[25] Yafet Y 1980 *Phys. Rev.* B **21** 5023
[26] Papaconstantopoulos D A 1986 *The Handbook of the Band Structure of Elemental Solids* (New York: Plenum)
[27] Lander J J 1953 *Phys. Rev.* B **91** 1382
[28] Fuggle J C and Mårtensson N 1980 *J. Electron Spectrosc. Relat. Phenom.* **21** 275
[29] Yin L I, Tsang T and Adler I 1977 *Phys. Rev.* B **15** 2974
[30] Antonides E, Janse E C and Sawatzky G A 1977 *Phys. Rev.* B **15** 1669
[31] de Boer D K G, Haas C and Sawatzky G A 1984 *J. Phys. F: Met. Phys.* **14** 2769